Poloidal density asymmetries due to ion cyclotron resonance heating

Ye.O. Kazakov[1], T. Fülöp[1], I. Pusztai[1], T. Johnson[2]

[1] *Department of Applied Physics, Chalmers University of Technology, Euratom-VR Association, Göteborg, Sweden*

[2] *School of Electrical Engineering, Royal Institute of Technology, Euratom-VR Association, Stockholm, Sweden*

Introduction Ion cyclotron resonance heating (ICRH) is one of the heating methods widely used in fusion devices. In connection with ICRH, poloidally asymmetric impurity distributions are often observed [1, 2], which may influence significantly the impurity cross-field transport. When low magnetic field side (LFS) ICRH heating is applied, impurities tend to accumulate on the *inboard* side of the flux surfaces, which may lead to outward impurity flux [3].

In the present work, the poloidal asymmetry of impurities in ICRH-heated tokamak plasmas is analyzed and the link between the asymmetry strength and the ICRH parameters is quantified. One of the main parameters governing the impurity asymmetry strength is the minority ion temperature anisotropy. Using TORIC-SSFPQL modelling [4], we analyze its dependence on plasma and ICRH parameters, specifically on heating power, central plasma density, fast wave toroidal wave number and impurity concentration.

Poloidal dependence of the minority density The minority heating (MH) scheme is the most commonly used ICRH scenario in tokamaks. It typically requires minority concentrations of a few percent to achieve efficient heating. The radio frequency (RF) power is absorbed dominantly by a small population of minority ions at the fundamental cyclotron resonance layer. MH is known to give rise to very energetic tails, accelerating the minorities preferentially in the perpendicular to the magnetic field direction. The distribution function for minority ions heated by ICRH could be modelled by the following ansatz [5]

$$f_{\rm m}(\mathcal{E},\mu,r) = \left(\frac{m_{\rm m}}{2\pi}\right)^{3/2} \frac{n_c(r)}{T_\perp(r)T_\parallel^{1/2}(r)} \exp\left[-\frac{\mu B_c}{T_\perp(r)} - \frac{|\mathcal{E}-\mu B_c|}{T_\parallel(r)}\right], \tag{1}$$

where $\mathcal{E} = m_{\rm m}v^2/2$, $\mu = m_{\rm m}v_\perp^2/(2B)$, B_c is the magnetic field at the ICRH resonance. Using this model we can derive approximate analytical expressions for the poloidal variation of the minority density to make its parametric dependences more explicit. We consider LFS ICRH heating and assume a simplified magnetic geometry with circular flux surfaces. For magnetic surfaces, which the ICRH resonance does not intersect, the poloidally varying minority density can be written as

$$n_{\rm m}(\theta) \simeq n_e X_{\rm m}\left[1 + k\cos\theta + (k^2/2)\cos(2\theta) + \ldots\right], \qquad k = \frac{\epsilon b_c(\alpha_T - 1)}{b_c + \alpha_T(1-b_c)}, \tag{2}$$

where $X_\mathrm{m} = \langle n_\mathrm{m} \rangle / n_e$ is the flux surface averaged minority concentration, $\epsilon = r_0/R_0$, $b_c = B_c/B_0$, and $\alpha_T = T_\perp/T_\parallel$ is the minority temperature anisotropy. The temperature anisotropy α_T can easily reach values around 10 if the ICRH power is sufficiently high and plasma density is low.

Minority temperature anisotropy In a classical paper by Stix [6], an approximate analytical solution is derived for the steady-state distribution function of minority ions heated at the fundamental cyclotron frequency. The minority distribution can be decomposed to the sum of the 'thermal' part and high-energy tail. The energies reached by the tail ions depend on a balance between the quasilinear RF heating term and the collisional term. The effective perpendicular temperature of the minorities is expected to be between the asymptotic values for the isotropic and anisotropic approximations considered by Stix

$$T_\perp^{(\mathrm{iso})} = T_e(1+\xi) < T_\perp < T_\perp^{(\mathrm{aniso})} = T_e(1+3\xi/2), \tag{3}$$

where the Stix parameter $\xi = (m_\mathrm{m} \langle P_\mathrm{RF} \rangle v_{te}) / \left(8\sqrt{\pi} X_\mathrm{m} n_e^2 Z_\mathrm{m}^2 e^4 \ln\Lambda\right)$, and $\langle P_\mathrm{RF} \rangle$ is the local volume averaged ICRH power absorbed by minority ions. Within the anisotropic approximation, the parallel tail temperature can be estimated as [6]

$$T_\parallel \simeq 5.9\, T_e\, A_\mathrm{m}^{1/3} Z_\mathrm{eff}^{2/3}. \tag{4}$$

In the present paper, the numerical method to assess the minority temperature anisotropy relies on computing the heating power deposition profiles using the full-wave 2D ICRH code TORIC [4], the output of which is then used to evaluate the minority distribution function with the simplified Fokker-Planck solver SSFPQL.

Baseline ICRH scenario We consider hydrogen minority heating in deuterium plasma $(X[\mathrm{H}] = 5\%)$, $R_0 = 3.0\,\mathrm{m}$, $a = 0.9\,\mathrm{m}$, $B_0 = 3.0\,\mathrm{T}$, $f = 41.2\,\mathrm{MHz}$, $n_\mathrm{tor} = 27$, $P_\mathrm{ICRH} = 3.0$ MW, $n_{e0} = 3.6 \times 10^{19}\,\mathrm{m}^{-3}$, $T_{e0} = T_{i0} = 5.0\,\mathrm{keV}$. This choice of the magnetic field and antenna frequency locates the fundamental resonance layer of hydrogen ions at the LFS, $R_\mathrm{H} = 3.33\,\mathrm{m}$.

Figure 1 shows the 2D minority ion absorption profiles calculated with TORIC [4] and SELFO [7] codes. Most of the RF power in (H)-D heating scenario is absorbed by the hydrogen minority: 87% and 92% predicted by TORIC and SELFO, respectively. By comparing TORIC and SELFO deposition profiles, one can conclude that the SELFO profile is broader (Fig. 1(c)). The origin of this difference is that the TORIC simulations were made assuming the Maxwellian distribution for all plasma species, including the heated minorities, while SELFO computes the deposition profiles and the change in the distribution function self-consistently. In addition, SELFO accounts for the finite orbit width effects, whereas TORIC-SSFPQL relies on the zero banana width approximation. However, the averaged power density and, consequently, the averaged minority perpendicular temperature within the radial range $r/a = [0.2 - 0.4]$ are comparable for the two different numerical approaches, $\langle T_\perp \rangle \simeq [150-160]\,\mathrm{keV}$. The parallel tail temperature given by TORIC-SSFPQL agrees quantitatively with the analytical estimate given by Eq. (4). For the parameters considered the tail parallel temperature at the heating maximum raises to $T_\| \simeq [20-25]\,\mathrm{keV}$.

Simulation results The minority temperature anisotropy depends on the plasma and ICRH parameters. It increases almost linearly with the input ICRH heating power. As Fig. 2(a) shows, α_T decreases significantly for higher central plasma densities. This is consistent with the fact that the parameter ξ, which defines the perpendicular minority temperature, is inversely proportional to the square of electron density. However, the numerical results presented in Fig. 2(a) exhibit a non-monotonic dependence on the plasma density, oscillating about the fitted curve. This oscillatory behaviour is probably due to the constructive/destructive interference, an effect that is well-known in 1D geometry. If the interference effect is to occur, then it should also be manifested in a scan over the fast wave toroidal wave number. This is indeed the case, as Fig. 2(b) illustrates: the minority temperature anisotropy depends non-monotonically on n_{tor}, with a pronounced oscillatory behaviour in the range $n_{\mathrm{tor}} > 20$, while as an overall trend, the anisotropy decreases for higher values of n_{tor}. The reason for this is that, in the case of the strong damping in a tokamak plasma (note that (H)-D scenario has very high single-pass absorption, typically $\sim 90\%$), the power deposition is controlled mostly by the Doppler broadening of the cyclotron resonance. Thus, the local RF power density achieved for higher n_{tor} is smaller since the absorption region is broader.

The minority temperature anisotropy also depends on the level of impurity contamination. Higher impurity concentrations give higher Z_{eff}, leading to an increase in the parallel temperature, according to Eq. (4). Fitting the data in Fig. 2(c), which is calculated for Be^{4+} impurity, gives the power exponent in Z_{eff}-dependence of the minority temperature anisotropy, $\alpha_T \propto Z_{\mathrm{eff}}^{-k_Z}$, to be $k_Z = 0.78$ for the maximum and $k_Z = 0.72$ for the averaged anisotropy, which is in a good agreement with the value $2/3$ obtained in the simplified model of Stix.

Impurity asymmetry strength The main reason for the impurity asymmetries driven by LFS ICRH is the increase of the minority density on the outboard side of the magnetic surface due to the trapping of the heated minority ions. The poloidal asymmetry of the minority density gives rise to an electrostatic field that pushes impurities to the opposite *(inboard)* side:

$$\frac{\delta n_z}{n_{z0}} \approx -\frac{Ze\phi_E}{T_z} \approx -\kappa\cos\theta, \qquad \kappa \approx \frac{ZX_{\mathrm{H}}\,k}{(T_z/T_{\mathrm{D}})X_{\mathrm{D}} + T_z/T_e + Z^2 X_z}. \tag{5}$$

The impurity asymmetry strength depends on the minority and impurity concentrations, impurity charge number, and also on the parameter k (Eq. (2)) that includes the minority temperature anisotropy. Its dependence on ICRH power is presented in Fig. 3 calculated for

$X[\mathrm{H}] = 8\%$. It is clearly seen that the largest impurity asymmetry is obtained in the trace limit.

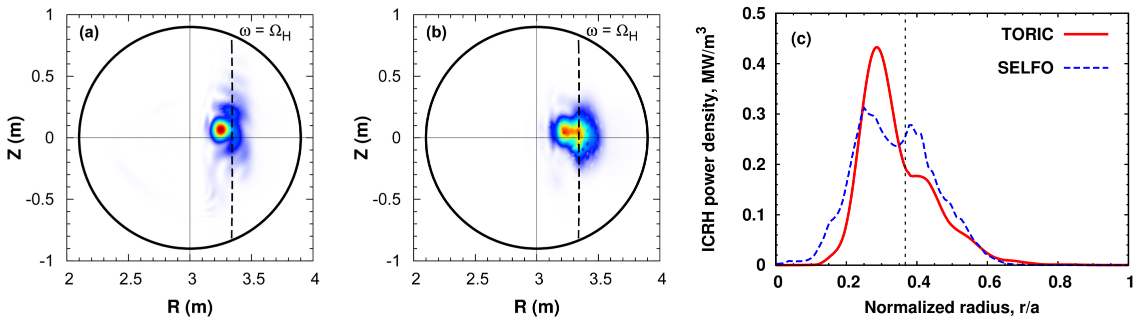

Figure 1: *2D profiles of RF power absorption by hydrogen minority ions calculated with TORIC (a) and SELFO (b) codes; Fig. 1(c) shows the flux surface averaged absorption profiles.*

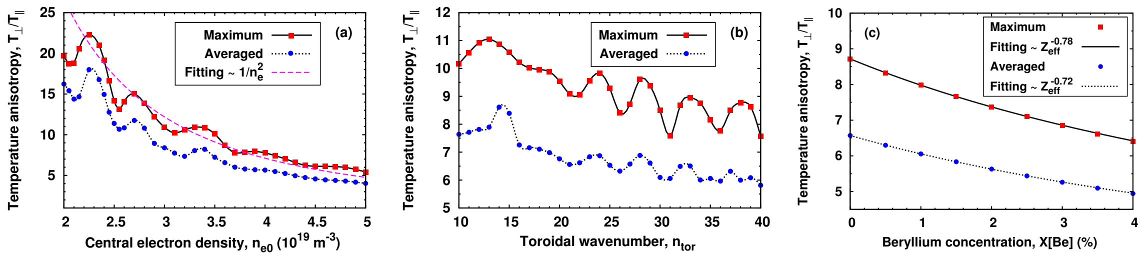

Figure 2: *Minority temperature anisotropy dependences evaluated with TORIC-SSFPQL.*

Conclusions Minority ion temperature anisotropy is identified to be one of the main parameters governing the 'in-out' poloidal impurity asymmetries observed under LFS ICRH heating. By means of TORIC-SSFPQL modelling, its dependence on the plasma and ICRH parameters is analyzed. A qualitative analytical estimate for the impurity asymmetry strength is obtained. Studying the relation between impurity asymmetries and ICRH is valuable not only for understanding the changes in the cross-field transport, but also for the possibilities to use the asymmetry measurements as diagnostics.

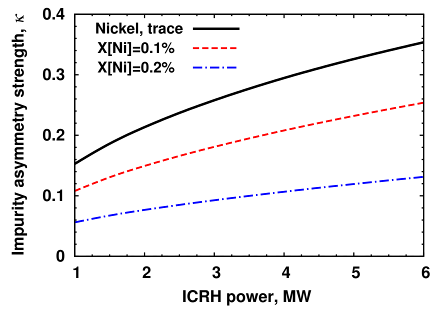

Figure 3: *Asymmetry strength for* Ni^{28+} *impurities as a function of ICRH power.*

Acknowledgments The authors are grateful to Dr. M. Brambilla and Dr. R. Bilato for providing the TORIC-SSFPQL code. This work was funded by the European Communities under Association Contract between EURATOM and *Vetenskapsrådet*.

[1] L.C. Ingesson, H. Chen, P. Helander and M.J. Mantsinen 2000 *Plasma Phys. Control. Fusion* **42** 161.

[2] M.L. Reinke, I.H. Hutchinson, J.E. Rice et al. 2012 *Plasma Phys. Control. Fusion* **54** 045004.

[3] A. Mollén, I. Pusztai, T. Fülöp, Ye.O. Kazakov, S. Moradi 2012 *Phys. Plasmas* **19** 052307.

[4] M. Brambilla and R. Bilato 2009 *Nucl. Fusion* **49** 085004.

[5] R.O. Dendy, R.J. Hastie, K.G. McClements and T.J. Martin 1995 *Phys. Plasmas* **2** 1623.

[6] T.H. Stix 1975 *Nucl. Fusion* **15** 737.

[7] J. Hedin, T. Hellsten, L.-G. Eriksson, T. Johnson 2002 *Nucl. Fusion* **42** 527.